The effect of turbulent flow structures on saltation sand transport in the atmospheric boundary layer

Sterk, G.; Jacobs, A.F.G.; van Boxel, J.

DOI
10.1002/(SICI)1096-9837(199810)23:10<877::AID-ESP905>3.0.CO;2-R

Publication date
1998

Document Version
Final published version

Published in
Earth Surface Processes and Landforms

Earth Surface Processes and Landforms
Earth Surf. Process. Landforms, **23**, 877–887 (1998)

THE EFFECT OF TURBULENT FLOW STRUCTURES ON SALTATION SAND TRANSPORT IN THE ATMOSPHERIC BOUNDARY LAYER

G. STERK[1]*, A. F. G. JACOBS[2] and J. H. VAN BOXEL[3]

[1]*Dept of Irrigation and Soil and Water Conservation, Wageningen Agricultural University, Nieuwe Kanaal 11, 6709 PA Wageningen, The Netherlands*
[2]*Dept of Meteorology, Wageningen Agricultural University, Duivendaal 2, 6701 AP Wageningen, The Netherlands*
[3]*Dept of Physical Geography and Soil Science, University of Amsterdam, Nieuwe Prinsengracht 130, 1018 VZ Amsterdam, The Netherlands*

Received 1 April 1996; 20 May 1997; Accepted 21 January 1998

ABSTRACT

The effect of turbulent flow structures on saltation sand transport was studied during two convective storms in Niger, West Africa. Continuous, synchronous measurements of saltation fluxes and turbulent velocity fluctuations were made with a sampling frequency of 1 Hz. The shear stress production was determined from the vertical and streamwise velocity fluctuations. The greatest stress-bearing events were classified as turbulent structures, with sweep, ejection, inward interaction, and outward interaction described according to the quadrant technique. The classified turbulent structures accounted for 63·5 per cent of the average shear stress during the first storm, and 56·0 per cent during the second storm. The percentage of active time was only 20·6 per cent and 15·8 per cent, respectively. High saltation fluxes were associated with sweeps and outward interactions. These two structures contribute positively (sweeps) and negatively (outward interactions) to the shear stress, but have in common that the streamwise velocity component is higher than average. Therefore, the horizontal drag force seems primarily responsible for saltation sand transport, and not the shear stress. This was also reflected by the low correlation coefficients (r) between shear stress and saltation flux (0·12 and 0·14, respectively), while the correlation coefficients between the streamwise velocity component and saltation flux were much higher (0·65 and 0·57, respectively).

KEY WORDS: turbulent flow structures; quadrant technique; shear stress; saltation transport

INTRODUCTION

A turbulent flow over a solid surface imparts instantaneous and localized levels of shear stress to the fluid–solid interface which are well above the average flow shear stress (Nearing and Parker, 1994). For example, Lapointe (1992) found that 80 per cent of the total shear stress exerted by water in the Fraser River (British Colombia, Canada) could be attributed to isolated events of 3 to 8 s duration, which occupied only 12 per cent of the time. The short events were identified as ejection and inrush structures of the turbulent bursting mechanism.

These turbulent structures can be defined by using horizontal and vertical turbulent velocity fluctuations. The instantaneous streamwise velocity u can be partitioned into a time average $\overline{u}$ and a turbulent fluctuating part u', superposed on the average. The same can be done for the vertical velocity component v. In Figure 1, four different turbulent structures are defined based on the quadrant technique (Wallace *et al.*, 1972). An ejection is an upward movement of low-velocity fluid from near the solid surface ($u'<0$, $v'>0$), while a downward movement of high-velocity fluid towards the solid surface ($u'>0$, $v'<0$) is called inrush or sweep. Both events result in a downward momentum transport and, hence, a positive contribution to the turbulent shear stress or Reynolds stress. In addition, two weaker motions, inward and outward interactions, exist. An outward interaction is an upward movement of high-velocity fluid ($u'>0$, $v'>0$), and an inward interaction is a downward movement of low-velocity fluid ($u'<0$, $v'<0$). Both events result in an upward momentum transport

* Correspondence to: Dr G. Sterk, Department of Irrigation and Soil and Water Conservation, Wageningen Agricultural University, Nieuwe Kanaal 11, 6709 PA Wageningen, The Netherlands.

CCC 0197-9337/98/100877–11 $17.50

and contribute negatively to the shear stress. For realistic flows, a positive shear stress exists. So, on average the absolute magnitude of the negative contributions has to be lower than the positive contributions given by ejections and sweeps (Lu and Willmarth, 1973).

Ejection and sweeps have often been associated with detachment and transportation of sediment. Sweeps are usually associated with the initiation and movement of bed-load transport (saltation + creep), whereas ejections are supposed to be more effective in lifting fine suspended material away from the surface (Dyer, 1986). The present knowledge of the links between the turbulent structures and sediment transport dynamics was mainly obtained from investigations in water flow, usually under laboratory conditions (e.g. Sutherland, 1967; Müller *et al*., 1971; Sumer and Oguz, 1978; Sumer and Deigaard, 1981; Grass, 1983), but also in geophysical boundary layers (e.g. Heathershaw and Thorne, 1985; Thorne *et al*., 1989; Lapointe, 1992). These geophysical studies have confirmed the relation between (i) ejections and suspension transport (Lapointe, 1992), and (ii) sweeps and bed-load transport (Heathershaw and Thorne, 1985; Thorne *et al*., 1989). In addition, the latter two studies revealed that outward interactions, although weaker and less frequent than sweeps, were capable of supporting bed-load movement as well. Heathershaw and Thorne (1985) hypothesized that shear stress is a necessary but not sufficient condition for bed-load transport, and that form drag on individual particles may have greater dynamic significance than the shear stress. This suggests that calculations of bed-load transport should not be based on shear stress alone, as many of the equations predicting bed-load transport rates in water flow generally are (Dyer, 1986; Julien, 1995).

Although much of relevance to sediment transport in turbulent airflows can be gleaned from the studies in aqueous environments, by comparison the role of turbulence in wind-blown particle transport has received very little attention (Butterfield, 1993). From a few wind tunnel studies, the importance of turbulence for entrainment of particles has been inferred (e.g. Bisal and Nielsen, 1962; Lyles and Krauss, 1971; Braaten *et al*., 1990), and three wind tunnel studies (Butterfield, 1991, 1993; Hardisty, 1993) provide data of instantaneous wind speed and sediment transport. Reports of field experiments are even more scarce. Only two studies were found (Lee, 1987; Butterfield, 1991). In none of these wind tunnel and field studies were the different turbulent structures identified to reveal their significance for wind-blown particle transport.

A better understanding of the wind erosion process, for instance for modelling purposes, requires detailed measurements of particle transport in relation to the turbulent wind flow, both under laboratory and natural circumstances (Bagnold, 1973). According to Butterfield (1993), it is essential that both mass flux and wind velocity histories are characterized to frequencies of at least 1 Hz if realistic and environmentally useful sediment transport relations are to be derived. In this study, data of synchronous measurements of turbulent velocity components and saltation sand transport during convective storms in the West African Sahel were collected. Only saltation transport was measured, because it is generally more easily quantified than creep and suspension transport. Furthermore, saltation is considered to initiate transport by the other two modes (Shao *et al*., 1993). So, understanding the saltation process also gives insight into creep and suspension transport. The objectives of the study were (i) to determine the magnitude and duration of peak Reynolds stresses, and (ii) to investigate the saltation response to velocity and shear stress fluctuations created by turbulent structures.

MATERIALS AND METHODS

Study site

A field experiment was conducted at the International Crops Research Institute for the Semi-Arid Tropics (ICRISAT) Sahelian Centre in southwest Niger (13°16′N, 2°21′E), during the rainy seasons of 1994 and 1995. The climate of the region is typical Sahelian, with one short (four months) rainy season and high temperatures all year round. In the early rainy season (May–July), large cumulonimbus clouds develop throughout the Sahel and bring the first rains of the new season. Those clouds are often accompanied by short (10–30 min) wind storms that precede rainfall. The storms are the result of strong downdrafts within the cloud that cause a forward outflow of cold air. The violent winds may create a spectacular rolling dust cloud that moves in front of the cumulonimbus cloud. In general, the cumulonimbus clouds move from east to west and the resulting wind direction during storms is expected to be easterly.

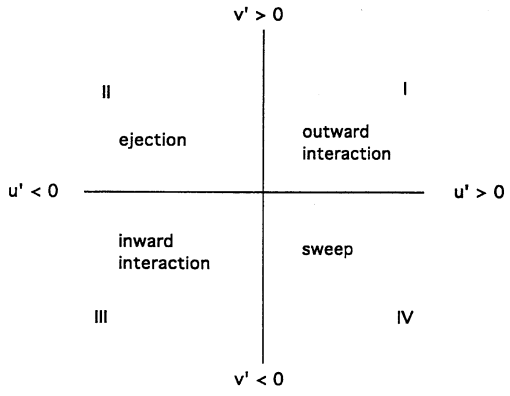

Figure 1. Quadrant plot of four discrete momentum exchange structures, based on the turbulent velocity fluctuations in horizontal (u') and vertical (v') directions

Table I. Aggregate size distribution of topsoil at ICRISAT Sahelian Centre

Size class (μm)	Mass (%)
<63	3·1
63–125	18·2
125–250	35·7
250–500	32·8
500–1000	10·0
>1000	0·2

The field used for the experiment was 90 m by 90 m in size. It was bordered by dirt roads at the northern and eastern sides, by a field protected against wind erosion with crop residues to the south, and by a wind break on the western side. The equipment was positioned such that distances from instruments to the field boundaries exceeded 50 m in the northern and eastern directions, and about 40 m in the southern and western directions. The whole field was planted with pearl millet (*Pennisetum glaucum*) on 17 June 1994 and 21 June 1995. Sowing was done according to the traditional Sahelian method, with sowing holes, or pockets, at wide spacings of 1 m by 1 m. In each hole approximately 50 to 100 seeds were thrown. Three weeks after sowing, the number of plants in each pocket was manually reduced to three.

The soil at the measurement field is a sandy alfisol with 92·2 per cent sand, 3·0 per cent silt and 4·8 per cent clay in the topsoil. The aggregate size distribution, determined by dry sieving of soil samples, is given in Table I. These sandy soils are very prone to crust formation by high-intensity rainfall in the early rainy season. Strong structural crusts are formed that have typically two layers (Valentin and Bresson, 1992). At some depth (5–10 mm), a thin and dense plasmic layer exists, which consists of fine particles (clay, silt and fine sand) that were washed out from the top layer. The top layer consists of loose, cohesionless sand, which is easily eroded by wind or water. Such a crust existed all the time in the field during the experiments. It was broken by weeding only twice per season, but returned immediately during the next rain.

The soil surface was smooth and without any roughness other than that created by the soil particles themselves, characterized by an average roughness height in the order of 0·001 m. Just after weeding the average roughness height increased to approximately 0·01 m, but in both seasons, no wind storms occurred during these periods. The roughness created by young millet plants was negligible during the first four weeks after sowing. The limited size of the plants (<0·10 m) and the low planting density assured that saltation transport was not significantly influenced by the crop. Surrounding the field, obstacles such as trees and bushes were present. During storms, the upwind distances from the measurement location to the obstacles exceeded in all cases 20 times the height of the obstacle. It was therefore assumed that the wind field at the measurement

location was not significantly disturbed by those obstacles. Saltating sand entering the field was not observed, but suspended dust from other areas was clearly moving into the field during periods of strong storms.

Measurements

Wind speed was recorded with a Gill UVW propeller anemometer (R.M. Young Co., model 27005), which measures three orthogonal components (*U, V* and *W*) of the wind vector (*F*). It consists of propellers with a diameter of 0·22 m, attached to the anemometer by shaft extension with a length of 0·45 m. The range of wind speeds that can be measured is from 0·3 to 25·0 m s^{-1}.

A propeller responds only to that component of the wind vector which is parallel to its axis of rotation. Off-axis response closely approximates a cosine curve, and the propeller does not rotate when wind flow is perpendicular to its axis (Hicks, 1972). The response time of the propellers is defined as the distance constant divided by the wind speed (Fichtl and Kumar, 1974). Use was made of expanded polystyrene propellers, which have a distance constant of 1·0 m (R.M. Young Co.). Hence, the response times of the three propellers are U^{-1}, V^{-1} and W^{-1} (s).

The anemometer was installed at 3 m above the soil surface, which means that the horizontal components *U* and *W* were measured at 2·95 and 3·05 m, respectively, and the vertical component *V* at 3·45 m. The analogue DC voltage signals of the three sensors were sampled at a frequency of 1 Hz with a CR10 data logger (Campbell Scientific Ltd). Since the anemometer was new, it was not calibrated prior to field installation. The recorded signals were converted to wind speeds by using the calibration constant given by the manufacturer.

Saltation transport was measured with the saltiphone, which is a robust saltation sensor that records particle impacts with a microphone. A detailed description of the device was given by Spaan and Van den Abeele (1991). It consists (Figure 2) of a microphone with a membrane of 201 mm^2, placed inside a stainless steel tube (diameter = 0·05 m, length = 0·13 m). The tube is mounted on a ball-bearing and is continuously positioned into the wind by two vanes at the back.

Some of the soil particles moving through the tube hit the membrane of the microphone. The frequency of the signals created depends on the momentum of the impacting particles. High frequency signals are formed by high momentum particles, like saltating sand grains. By amplifying high frequencies and filtering low frequencies, the signals created by saltating sand can be distinguished from other noises, created for instance by wind or suspended dust. The amplified signal of a particle impact produces a pulse that is cut off after 1 ms. Each time a pulse is generated, no other particle impact can be detected. So, theoretically, the maximum number of particle impacts that can be detected is 1000 per second. The actual number of particle impacts can be higher than the number of counted pulses, due to overlap of particle impacts during the same pulse. The output of the saltiphone (*S*) in counts per unit of time, therefore, is a relative measure of the saltation flux at the height of the microphone. Wind tunnel tests with the saltiphone (Sterk, 1993) showed that the pulse count rate is linearly related to the measured mass flux at the same height (Figure 3). However, the range of mass fluxes during those experiments was somewhat narrow, and it is uncertain whether the relationship is still valid for higher and lower fluxes.

Three saltiphones were installed in the field. All three sensors were positioned around the UVW anemometer, at 2·0 m from the mast in the north, east and south directions. The height of the centre of the microphones above the soil surface was 0·10 m. The saltiphones were connected to a pulse count expansion (SDM-SW8A) on the CR10 data logger. The maximum input frequency of the SDM-SW8A pulse channels is 100 Hz, which is not sufficient for the saltiphone. In order to reduce the number of incoming pulses, a self-constructed pulse divider was placed between the saltiphone and the data logger. Of every ten incoming pulses, nine were filtered and only one was sent to the data logger. In the output, the number of pulses was multiplied again by ten. Furthermore, an automatic rain gauge (tipping-bucket) was installed to determine the exact moment of onset of rainfall. Like the UW anemometer, the saltiphones and rain gauge were also sampled at a frequency of 1 Hz.

Analytical procedure

From the three measured wind components *U, V* and *W*, the instantaneous wind vector *F* and its direction ω were calculated, with ω being the angle of *F* relative to the north. The mean wind vector $\overline{F}$ and its direction $\overline{\omega}$

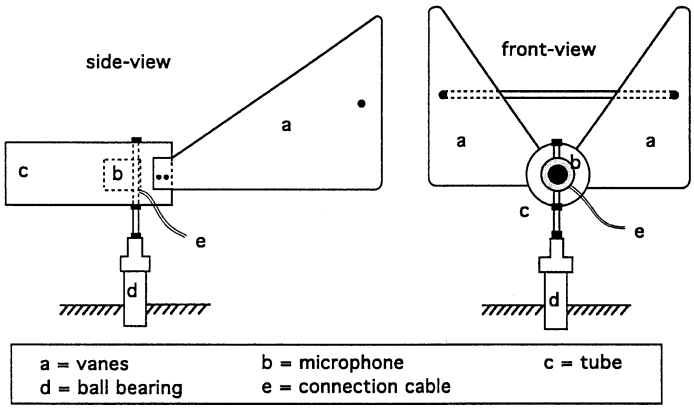

Figure 2. The saltiphone

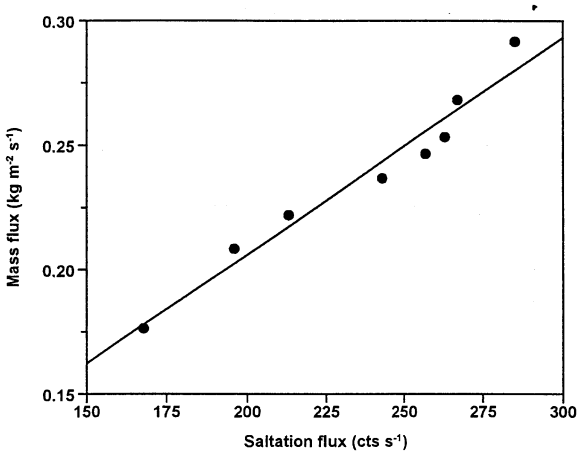

Figure 3. Relationship between saltation flux, measured with a saltiphone, and mass flux, measured with a sediment trap in a wind tunnel

were calculated for the storm duration, or for periods of 10 min, in the case of storms with long duration. A new orthogonal coordinate system was chosen with the positive x-axis parallel to the surface in the direction $\overline{\omega}$ of the mean flow $\overline{F}$, the positive y-axis normal to the surface in an upward direction, and the positive z-axis parallel to the surface to the right of the positive x-axis. The instantaneous velocity components U, V and W were converted to the new components u, v and w, with u being the instantaneous velocity parallel with x, v the instantaneous velocity parallel with y, and w the instantaneous velocity parallel with z.

The instantaneous velocity components were decomposed into an average and a fluctuating, turbulent part: $u=\overline{u}+u'$; $v=\overline{v}+v'$; $w=\overline{w}+w'$. By definition, $\overline{w}$ is zero, whereas $\overline{v}$ will be close to, but not necessarily equal to, zero. Within a convective storm moving ahead of a cumulonimbus cloud, strong updrafts exist that locally result in a positive $\overline{v}$ component. Moreover, the wind flow is also slightly pushed upward by the anemometer, resulting in a positive $\overline{v}$ component, but this effect is reduced to a minimum by the vertical shaft extension on the UVW anemometer.

The time-average velocity fluctuations $\overline{u'}$, $\overline{v'}$ and $\overline{w'}$ are zero by definition. The time-averages of the squares and mixed products, however, are non-zero, and create the Reynolds stresses. The average stress component, $\overline{\tau}_{xy}=-\rho\,\overline{u'v'}$ (N m^{-2}), gives the streamwise shear stress in a horizontal plane, and is usually considered to be directly related to sediment transport dynamics. Dividing the shear stress by the fluid density (ρ) gives the average kinematic stress $-\overline{u'v'}$ (m^2 s^{-2}), while the instantaneous values of kinematic stress are represented by $-u'v'$ (Allen, 1994). In the following sections of this paper, emphasis will be placed on the instantaneous and average values of the streamwise kinematic stress.

Table II. Descriptive statistics* of wind parameters and saltation transport during two storms at ICRISAT Sahelian Centre

	27 June 1994					25 June 1995				
	F ($m s^{-1}$)	u' ($m s^{-1}$)	v' ($m s^{-1}$)	$-u'v'$ ($m^2 s^{-2}$)	S ($cts s^{-1}$)	F ($m s^{-1}$)	u' ($m s^{-1}$)	v' ($m s^{-1}$)	$-u'v'$ ($m^2 s^{-2}$)	S ($cts s^{-1}$)
Mean	9·67	0	0	0·41	97·7	9·49	0	0	0·36	42·4
Median	9·45	–0·22	0·02	0·09	40·0	9·41	–0·11	–0·03	0·11	10·0
Stand. dev.	2·31	2·33	0·62	1·49	119·4	2·15	2·15	0·57	1·23	66·5
Skewness	0·44	0·48	0·08	0·94	1·34	0·23	0·22	–0·08	2·17	2·53
Kurtosis	–0·31	–0·28	1·53	5·63	1·11	–0·57	–0·59	2·85	17·49	7·91
Range	12·63	12·65	5·37	15·44	520·0	10·94	10·75	5·59	18·39	480·0
Min.	4·59	–4·98	–2·71	–7·83	0	4·06	–5·35	–3·03	–6·82	0
Max.	17·22	7·68	2·66	7·62	520·0	15·00	5·39	2·56	11·57	480·0

* F is the wind speed; u' and v' are the horizontal and vertical turbulent velocity fluctuations; $-u'v'$ is the kinematic stress; S is the saltation flux

The four discrete categories of momentum exchange – ejection, sweep, inward interaction and outward interaction – were defined on the basis of the relative signs of u' and v' (Figure 1). In order to avoid the problem of assigning a discrete structure to individual low magnitude stress contributions purely on the basis of the values of u' and v', a threshold criterion was defined. Only those events that exceeded the average kinematic stress by at least one standard deviation (σ) were identified as structures. Thus, instantaneous contributions to the average kinematic stress in the interval $[-\bar{u}'\bar{v}', -\sigma, -\bar{u}'\bar{v}', +\sigma]$ were not assigned by a momentum exchange category from Figure 1.

RESULTS AND DISCUSSION

A total of 20 storms was recorded during the 1994 and 1995 rainy seasons. Of the collected data, only those periods with more or less continuous saltation transport and without rainfall were used for the analysis. Two typical storms on 27 June 1994 (storm 1) and 25 June 1995 (storm 2), both with a duration of about 10 min and nearly similar average wind speeds (Table II), were selected. During both storms the wind direction was east, hence the data from the saltiphone east of the UVW anemometer was used for the analysis.

Plots of recorded wind speed and saltation response are given for the two storms. In Figure 4, individual fluctuations in wind speed display a range of periods or frequencies in the tubulence spectrum. Low frequency oscillations with a periodicity of several minutes are evident as well as short gusts with a duration of 1 to 5 s. The size of the smallest quasi-horizontal structures or eddies that can be detected from the data is determined by the sampling frequency (1 Hz) and the average wind speed. The wavelength of the smallest detectable structures is equal to the average wind speed divided by the sampling frequency (Wieringa and Rijkoort, 1983). For both storms, the minimum size is approximately 9·5 m. Hence, it is assumed that the smallest quasi-horizontal eddies detected at 3 m height were large enough to cause at the same time strong horizontal velocity fluctuations near the soil surface. A detailed analysis of the turbulent frequency spectrum will be described in a separate paper. Here, emphasis is on the saltation response to wind speed and shear stress fluctuations.

The saltation flux was clearly intermittent in nature, with sporadic bursts of intense saltation transport immediately followed by periods without transport (Figure 4). The flow conditions during both storms were only slightly above threshold. As a result, saltation transport occurred only during gusts of varying durations. The saltation system responded quickly to wind speed fluctuations and, in general, a good relationship between instantaneous wind speed and saltation flux exists. Correlation coefficients (r) for wind speed and saltation count rate during the two storms are 0·65 and 0·57, respectively. The correlation coefficients are slightly better when the saltiphone recordings are assumed to lag 1 s behind wind speed (0·71 and 0·65). With an assumed lag of 2 s the correlation coefficients are 0·64 and 0·60, respectively, and decrease rapidly with increasing lag. The better correlation at a lag of 1 s indicates that the response time of the saltation system to reach steady state is in the order of 1 s. This result is in accordance with the response time as it was calculated from numerical simulations by Anderson and Haff (1988), and was confirmed by the experiments of Butterfield (1991). However, it seems likely that the response time obtained in this study was influenced by the height difference between saltiphone and anemometer. But it is assumed that this effect was negligible, since the gusts detected at 3 m were caused by structures large enough to cause at the same time strong gusts near the soil surface.

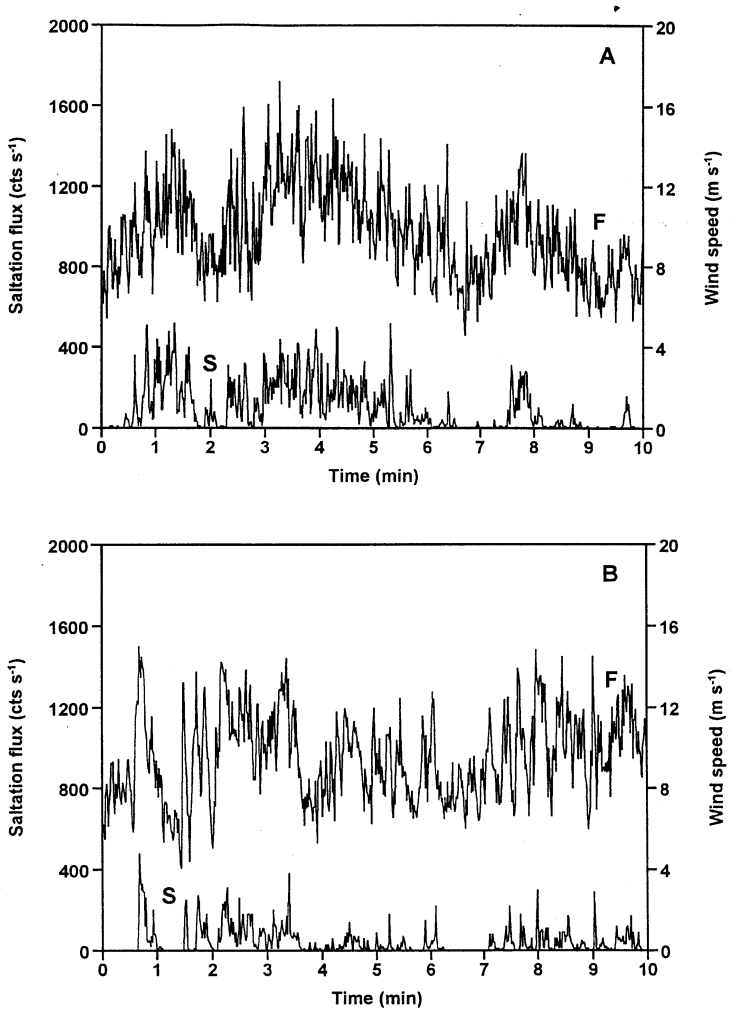

Figure 4. Records of wind speed (*F*) and saltation flux (*S*) for two Sahelian wind erosion events at ICRISAT Sahelian Centre on (A) 27 June 1994 and (B) 25 June 1995

From the data, the threshold wind speed conditions for initiation and cessation of saltation transport could be determined. The threshold wind speed at initiation of saltation was defined by Bagnold (1973) as the fluid threshold, i.e. the threshold at which sand movement starts owing to the direct force of the fluid only. The threshold wind speed at which saltation ceases is similar to Bagnold's impact threshold, defined as the threshold wind speed at which an initial disturbance of the sand becomes a continuous movement downwind. In other words, the wind alone is insufficient to initiate saltation transport, but saltation is sustained by the combined action of the wind force and the impacts of descending grains.

During both storms, periods of continuous saltation transport alternated with periods of no transport (Figure 4). By selecting each isolated period of continuous saltation, the wind velocities at initiation and cessation of saltation transport were determined. On average, saltation started at 8·48 m s^{-1} (fluid threshold) and ceased at 7·66 m s^{-1} (impact threshold) during the first storm. During the second storm, the average fluid threshold was 9·60 m s^{-1} and the impact threshold was equal to 8·45 m s^{-1}. The higher threshold conditions during the second storm can be explained by wetting of the topsoil due to a light rain (2·0 mm) some 36 h earlier. Soil moisture results in water films surrounding the soil particles which create cohesive forces between the particles. The wind force required to lift particles from a moist surface is therefore higher than during dry conditions (Chepil, 1956). This also explains the lower average saltation flux during the second storm (Table II).

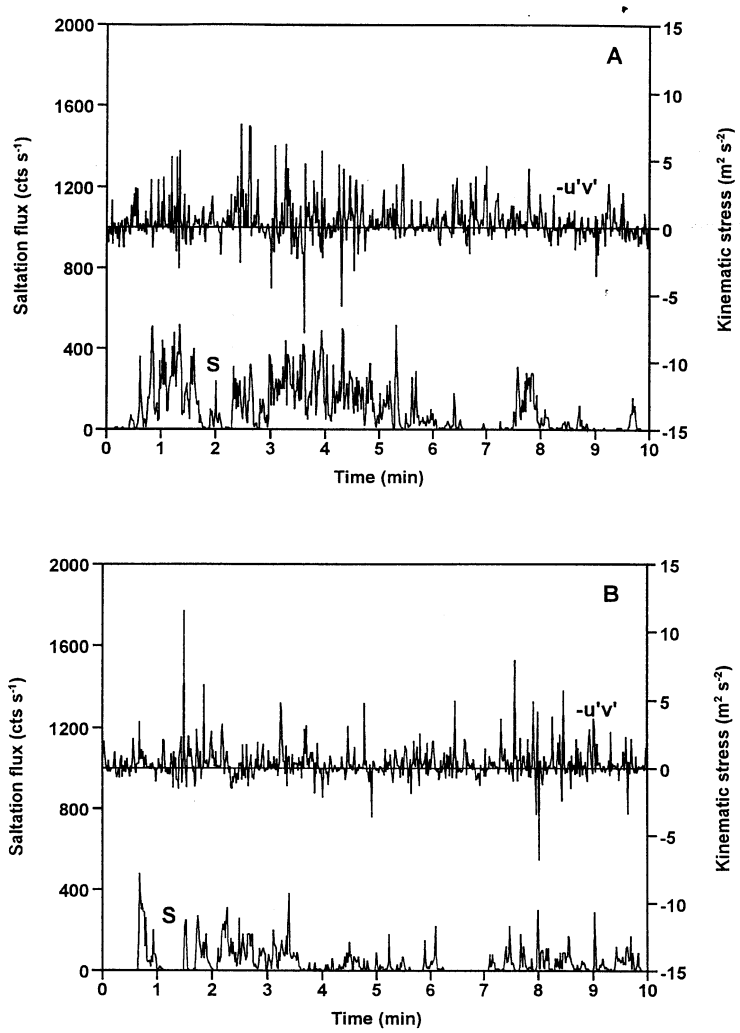

Figure 5. Plots of instantaneous kinematic stress ($-u'v'$) and saltation flux (S) for two Sahelian wind erosion events at ICRISAT Sahelian Centre on (A) 27 June 1994 and (B) 25 June 1995

Table III. Characteristics of four classified turbulent structures

Date	Number of events*				Mean duration (s)				Mean stress (m^2s^{-2})				Contribution to average stress (%)				Mean saltation flux ($cts\,s^{-1}$)			
	1	2	3	4	1	2	3	4	1	2	3	4	1	2	3	4	1	2	3	4
27/6/1994	19	24	21	31	1·32	1·42	1·10	1·35	–2·33	2·91	–1·54	3·65	–23·4	39·7	–14·3	61·5	256·8	23·2	19·6	241·7
25/6/1995	14	24	18	23	1·14	1·25	1·00	1·35	–1·92	2·67	–1·42	3·15	–14·2	36·9	–11·8	45·1	65·0	3·3	15·6	126·8

* 1= outward interaction; 2 = ejection; 3 = inward interaction; 4 = sweep

The instantaneous contributions to the average kinematic stress for both storms are shown in Figure 5. The average stress is the result of short but intense positive contributions, superposed on negative and weaker positive contributions. Instantaneous stress levels were 10 to 20 times stronger than the average stress level, but they occurred only during a very limited period of time. This intermittency in stress production occurs despite the fact that u' and v' are approximately Gaussian distributed (Table II) and randomly fluctuating quantities when taken separately. The small deviations from the normal distribution cause a non-normal distribution of the

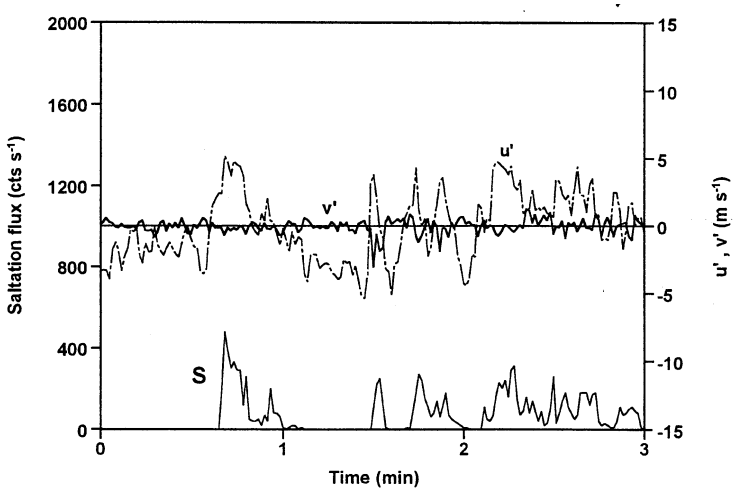

Figure 6. Saltation flux (S) in relation to horizontal (u') and vertical (v') turbulent velocity fluctuations during the first 3 min of a storm event at ICRISAT Sahelian Centre on 25 June 1995

kinematic stress, which is typical for turbulence (Panofsky and Dutton, 1984). The kinematic stress distribution is characterized by a positive skew (Table II), indicating a relatively frequent occurrence of extreme values.

The kinematic stress events that exceeded the average value by at least one standard deviation were classified as turbulent flow structures. Some characteristics of the structures are given in Table III. Of the average stress at sensor level, the classified structures accounted for 63·5 per cent during the first storm, and 56·0 per cent during the second storm. The percentage of time during which the structures were active was only 20·6 per cent for the first, and 15·8 per cent for the second storm. The number of sweeps and ejections was 41·6 per cent higher than the number of inward and outward interactions, and their positive contributions to the shear stress were about 56 per cent stronger than the total negative stress contributions, resulting in an overall positive shear stress.

A well-defined relationship between the instantaneous kinematic shear stress and saltation flux does not exist. The correlation coefficients for both storms are 0·12 and 0·14, respectively, and when the saltation flux is assumed to lag 1 s behind kinematic stress, the coefficients are 0·05 and 0·15, respectively. Also, no correlation between kinematic shear stress and saltation flux exists when only the time periods with classified turbulent structures are considered. However, mean saltation fluxes for the four classified structures (Table III) reveal that sweeps (class 4) and outward interactions (class 1) were associated with high saltation fluxes, whereas their stress contributions were positive and negative, respectively. Ejections (class 2) and inward interactions (class 3) were not capable of supporting appreciable saltation transport. Obviously, instantaneous contributions to the shear stress were of little significance in terms of saltation transport.

Sweeps and outward interactions have in common that u' is positive (Figure 1), meaning that the instantaneous horizontal wind speed is higher than average. Ejections and inward interactions have negative u' values, or lower than average horizontal wind speeds. Correlation coefficients between u' and saltation flux are exactly the same as the correlation coefficients given earlier between wind speed (F) and saltation flux (0·65 and 0·57), whereas the correlation between v' and saltation flux is weak (–0·18 and –0·22). This is also illustrated in Figure 6, where u', v' and the saltation flux during the first 3 min of the second storm are given. The close correspondence between u' and the saltation flux is clear. The value of v' tended to be negative during periods with saltation transport, but many exceptions can be found as well. These results suggest that the horizontal velocity fluctuations are of much more importance for saltation transport than the vertical velocity fluctuations.

In the foregoing analysis, instantaneous saltation flux was related to shear stress fluctuations measured at 3 m, assuming similar shear stress fluctuations being active near the soil surface at the same time. It is doubtful whether this assumption is correct. A similar assumption was made for the instantaneous wind speed, and the

minimum size (9·5 m) of detectable quasi-horizotal eddies indicates that this assumption was correct. Hence, positive u' values at 3 m were associated with positive values near the soil surface. A positive v' at 3 m does not necessarily mean that v' near the soil surface was positive as well. The vertical velocity fluctuations are produced by small eddies, with a diameter of the order of the height above the ground (Panofsky and Dutton, 1984). So, the observation of a downward moving eddy at 3 m does not necessarily mean that at the same time the shear stress created by the eddy was felt at the soil surface. Furthermore, such an eddy was moved horizontally with the average wind speed, which was an order of magnitude higher than the vertical wind speeds (Table II), resulting in shear stress at the soil surface downwind of the anemometer. This uncertainty may have obscured the shear stress–saltation flux relationship. For instance, the data presented here do not show an exclusive role of sweeps for the initiation of saltation movement, as suggested by Grass (1983). More detailed measurements of instantaneous shear stress near the soil surface would possibly reveal that sweeps are the principal structures associated with initiation of saltation transport.

Despite the uncertainty in the shear stress–saltation flux relationship, it is concluded that for saltation transport the horizontal wind speed component is of much more significance than the vertical component. Turbulent structures with a positive u' component, sweeps and outward interactions, are able to initiate and sustain saltation transport, whereas structures with a negative u' component do not. Apparently, it is not the streamwise shear stress component but the horizontal drag force, proportional to u^2, which is the driving force for saltation sand transport. The same was concluded for bed-load transport above a sea bed (Heathershaw and Thorne, 1985; Thorne *et al*. 1989). This conclusion suggests that saltation transport should not be predicted on the basis of shear stress (or friction velocity) alone, as most of the current transport equations are (Greeley and Iversen, 1985). It would be more useful if horizontal wind speed and its fluctuations, for instance described by the average and standard deviation, were incorporated in saltation transport models.

CONCLUSIONS

Measured fluxes of wind-blown saltation sand transport during two convective storms in the Sahelian zone of Niger showed a high degree of intermittency. Fluctuations in saltation flux were directly related to the gustiness of the wind. The best correlation between instantaneous wind speed and saltation flux was obtained when the measured saltation flux was assummed to lag 1 s behind wind speed. This result confirms that the response time of the saltation system is in the order of 1 s, as calculated by Anderson and Haff (1988).

During the two storms, classified turbulent structures accounted in isolation for 60 per cent of the average shear stress at sensor level, but the active time was only 18 per cent. Of the four turbulent structures that were distinguished by the quadrant technique (Figure 1), only sweeps and outward interactions were able to initiate and sustain saltation transport. Sweeps resulted in positive contributions to the average shear stress, whereas outward interactions contributed negatively to the average shear stress. The two structures have in common that the horizontal wind speed component was higher than average. It is not the streamwise shear stress, therefore, but the horizontal drag force that is primarily responsible for saltation sand transport. This result indicates that saltation transport models should incorporate the horizontal wind speed and its fluctuations as driving variables, instead of using the shear stress or friction velocity alone, as many of the current models do.

ACKNOWLEDGEMENTS

The research was funded by the Netherlands Foundation for the Advancement of Tropical Research (WOTRO). The logistic support of the ICRISAT Sahelian Centre is gratefully acknowledged. We thank Gijs van den Abeele of the Wageningen Agricultural University for his help with construction and installation of the electronic field equipment.

REFERENCES

Allen, J. R. L. 1994. 'Fundamental properties of fluids and their relation to sediment transport processes', in Pye, K. (Ed.), *Sediment Transport and Depositional Processes*, Blackwell Scientific Publication, Oxford, 25–60.

Anderson, R. S. and Haff, P. K. 1988. 'Simulation of eolian saltation', *Science*, **24**, 820–823.

Bagnold, R. A. 1973. *The Physics of Blown Sand and Desert Dunes*, 5th edn, Chapman and Hall, London.
Bisal, F. and Nielsen, K. F. 1962. 'Movement of soil particles in saltation', *Can. J. Soil Sci.*, **42**, 81–86.
Braaten, D. A., Paw, U. K. T. and Shaw, R. H. 1990. 'Particle resuspension in a turbulent boundary layer – observed and modeled', *J. Aerosol Sci.*, **21**, 613–628.
Butterfield, G. R. 1991. 'Grain trasport rates in steady and unsteady turbulent airflows', *Acta Mech. (Suppl.)*, **1**, 97–122.
Butterfield, G. R. 1993. 'Sand transport response to fluctuating wind velocity', in Clifford, N. J. *et al*. (Eds), *Turbulence: Perspectives on Flow and Sediment Transport*, John Wiley, Chichester, 303–335.
Chepil, W. S. 1956. 'Influence of moisture on erodibility of soil by wind', *Soil Sci. Soc. Am. Proc.*, **20**, 288–292.
Dyer, K. R. 1986. *Coastal and Estuarine Sediment Dynamics*, John Wiley, Chichester.
Fichtl, G. H. and Kumar, P. 1974. 'The response of a propeller anemometer to turbulent flow with the mean wind vector perpendicular to the axis of rotation', *Bound, Layer Meteor.*, **6**, 363–379.
Grass, A. J. 1983. 'The influence of boundary layer turbulence on the mechanics of sediment transport', in Sumer, B. M. and Müller, A. (Eds), *Mechanics of Sediment Transport. Proceedings Euromech 156*, Balkema, Rotterdam, The Netherlands, 3–18.
Greeley, R. and Iversen, J. D. 1985. *Wind as a Geological Process on Earth, Mars, Venus and Titan*, Cambridge University Press, Cambridge.
Hardisty, J. 1993. 'Frequency analysis of sand transport in a turbulent air flow', in Clifford, N. J. *et al*. (Eds), *Turbulence: Perspectives on Flow and Sediment Transport*, John Wiley, Chichester, 295–304.
Heathershaw, A. D. and Thorne, P. D. 1985. 'Sea-bed noises reveal the role of turbulent bursting phenomenon in sediment transport by tidal currents', *Nature*, **316**, 339–342.
Hicks, B. B. 1972. 'Propeller anemometers as sensors of atmospheric turbulence', *Bound. Layer Meteor.*, **3**, 214–228.
Julien, P. Y. 1995. *Erosion and Sedimentation*, Cambridge University Press, Cambridge.
Lapointe, M. 1992. 'Burst-like sediment suspension events in a sand bed river', *Earth Surf. Proc. Landforms*, **17**, 253–270.
Lee, J. A. 1987. 'A field experiment on the role of small scale wind gustiness in aeolian sand transport', *Earth Surf. Proc. Landforms*, **12**, 331–335.
Lu, S. S. and Wilmarth, W. W. 1973. 'Measurement of the structure of the Reynolds stress in a turbulent boundary layer', *J. Fluid Mech.*, **60**, 481–511.
Lyles, L. and Krauss, R. K. 1971. 'Threshold velocities and initial particle motion as influenced by air turbulence', *Trans. ASAE*, **14**, 563–566.
Müller, A., Gyr, A. and Dracos, T. 1971. 'Interactions of rotating elements of the boundary layer with grains of the bed: A contribution to the problem of the threshold of sediment transportation', *J. Hydraulic Res.*, **9**, 272–411.
Nearing, M. A. and Parker, S. C. 1994. 'Detachment of soil by flowing water under turbulent and laminar conditions', *Soil Sci. Soc. Am. J.*, **58**, 1612–1614.
Panofsky, H. A. and Dutton, J. A. 1984. *Atmospheric Turbulence: Models and Methods for Engineering Applications*, John Wiley, New York.
Shao, Y., Raupach, M. R. and Findlater, P. A. 1993. 'The effect of saltation bombardment on the entrainment of dust by wind', *J. Geophys. Res.*, **98**, 12 719–12 726.
Spaan, W. P. and Van den Abeele, G. D. 1991. 'Wind borne particle measurements with acoustic sensors', *Soil Technology*, **4**, 51–63.
Sterk, G. 1993. *Sahelian wind erosion research project, Report III. Description and calibration of sediment samplers*, Dept of Irrigation and Soil and Water Conservation, Wageningen Agricultural University, The Netherlands.
Sumer, B. M. and Deigaard, R. 1981. 'Particle motions near the bottom in turbulent flow in an open channel. Part 2', *J. Fluid Mech.*, **109**, 311–337.
Sumer, B. M. and Oguz, B. 1978. 'Particle motions near the bottom in turbulent flow in an open channel', *J. Fluid Mech.*, **86**, 109–127.
Sutherland, A. J. 1967. 'Proposed mechanism for sediment entrainment by turbulent flows', *J. Geophys. Res.*, **72**, 6183–6194.
Thorne, P. D., Williams, J. J. and Heathershaw, A. D. 1989. 'In situ acoustic measurements of marine gravel threshold and transport', *Sedimentology*, **36**, 61–74.
Valentin, C. and Bresson, L. M. 1992. 'Morphology, genesis and classification of surface crusts in loamy and sandy soils', *Geoderma*, **55**, 225–245.
Wallace, J. M. H., Eckelmann, H. and Brodkey, R. S. 1972. 'The wall region in turbulent shear flow', *J. Fluid Mech.*, **54**, 39–48.
Wieringa. J. and Rijkoort, P. J. 1983. *Wind-climate of The Netherlands*, Royal Dutch Meteorological Institute (KNMI), De Bilt, The Netherlands (in Dutch).

